© 2014. Published by The Company of Biologists Ltd | Journal of Cell Science (2014) 127, 3425–3433 doi:10.1242/jcs.149674

SHORT REPORT

PKA-regulated VASP phosphorylation promotes extrusion of transformed cells from the epithelium

Katarzyna A. Anton[1,2], John Sinclair[3], Atsuko Ohoka[4], Mihoko Kajita[4], Susumu Ishikawa[4], Peter M. Benz[5], Thomas Renne[6,7], Maria Balda[1], Claus Jorgensen[3,*], Karl Matter[1,‡] and Yasuyuki Fujita[2,4,‡]

ABSTRACT

At the early stages of carcinogenesis, transformation occurs in single cells within tissues. In an epithelial monolayer, such mutated cells are recognized by their normal neighbors and are often apically extruded. The apical extrusion requires cytoskeletal reorganization and changes in cell shape, but the molecular switches involved in the regulation of these processes are poorly understood. Here, using stable isotope labeling by amino acids in cell culture (SILAC)-based quantitative mass spectrometry, we have identified proteins that are modulated in transformed cells upon their interaction with normal cells. Phosphorylation of VASP at serine 239 is specifically upregulated in Ras^{V12}-transformed cells when they are surrounded by normal cells. VASP phosphorylation is required for the cell shape changes and apical extrusion of Ras-transformed cells. Furthermore, PKA is activated in Ras-transformed cells that are surrounded by normal cells, leading to VASP phosphorylation. These results indicate that the PKA–VASP pathway is a crucial regulator of tumor cell extrusion from the epithelium, and they shed light on the events occurring at the early stage of carcinogenesis.

KEY WORDS: Apical extrusion, Ras-transformed, VASP, PKA

INTRODUCTION

At the initial stage of carcinogenesis, oncogenic transformation occurs in a single cell within the epithelium. We have recently reported that Ras-transformed cells are apically extruded when surrounded by normal neighbors (Hogan et al., 2009). This phenomenon is shared by cells transformed with other oncogenes, such as v-Src, and occurs in both invertebrates and vertebrates *in vivo* (Kajita et al., 2010). The interaction with normal neighbors induces Ras-transformed cells to undergo changes in cell shape, resulting in increased cell height, and to remodel their actin cytoskeleton, leading to filamentous (F)-actin accumulation at cell–cell contacts (Hogan et al., 2009). However, the molecular mechanisms regulating these processes remain obscure. In particular, it is not clear what molecular switches are involved in the morphological changes of transformed cells that are required for extrusion. Uncovering the mechanism of apical extrusion is not only crucial for understanding early carcinogenesis, but it could shed light on the mechanics of other cell-sorting events that take place during development.

In this study, we used quantitative mass spectrometry to identify proteins that are modulated in transformed cells interacting with normal cells. Phosphorylation of VASP at serine 239 was specifically upregulated in Ras-transformed cells interacting with normal cells. VASP phosphorylation was required for the apical extrusion of Ras-transformed cells and occurred downstream of PKA. These results reveal a novel molecular mechanism controlling the elimination of transformed cells from the epithelium.

RESULTS AND DISCUSSION

SILAC screening for phosphorylation in Ras-transformed cells interacting with normal cells

To reveal the molecular mechanisms that occur during the apical extrusion of Ras-transformed cells surrounded by normal epithelial cells, we performed a quantitative mass spectrometric analysis (Jørgensen et al., 2009; Mann, 2006). Using stable isotope labeling with amino acids in cell culture (SILAC)-based quantitative proteomics, we examined phosphorylated proteins in transformed cells. We used Madin-Darby canine kidney (MDCK) cells expressing GFP-tagged constitutively active oncogenic Ras (Ras^{V12}) controlled by a tetracycline-inducible promoter (hereafter referred to as Ras cells) (Hogan et al., 2009). Three types of isotope-labeled arginine and lysine were used – heavy (Arg 10, Lys 8) and medium (Arg 6, Lys 4), for labeling Ras cells, and light (Arg 0, Lys 0) for normal untransfected MDCK cells (Fig. 1A). Heavy-labeled Ras cells were mixed with light-labeled MDCK cells, whereas medium-labeled Ras cells were cultured alone (Fig. 1A). Following a 6-h induction of Ras^{V12} expression with tetracycline, the cell lysates were combined and the amounts of heavy- and medium-labeled phosphorylated peptides were compared by quantitative mass spectrometry; the ratio of heavy to medium label (hereafter called the H:M ratio) was calculated for each peptide (Fig. 1B). For >35% of peptides identified, we were able to calculate the H:M ratio. Peptides with an H:M ratio of >1.5 or <0.5, reproduced in at least two out of three independent experiments, were considered as biologically relevant modifications (Fig. 1C; supplementary material Fig. S1). Over 80% of the H:M ratios were between 0.5 and 1.5, indicating that the phosphorylation status of most of the proteins was not significantly affected. In total, we identified 17 proteins that were more phosphorylated and 15 that were less phosphorylated in

[1]Department of Cell Biology, UCL Institute of Ophthalmology, University College London, London EC1V 9EL, UK. [2]MRC Laboratory for Molecular Cell Biology and Cell Biology Unit, University College London, London WC1E 6BT, UK. [3]Division of Cancer Biology, Cell Communication Team, The Institute of Cancer Research, London SW3 6JB, UK. [4]Division of Molecular Oncology, Institute for Genetic Medicine, Hokkaido University, Sapporo 060-0815, Japan. [5]Institute for Vascular Signaling, University of Frankfurt, Frankfurt D-60590, Germany. [6]Department of Molecular Medicine and Surgery and Center for Molecular Medicine, Karolinska Institute, Stockholm SE-171 77, Sweden. [7]Institute for Clinical Chemistry, University Hospital Hamburg-Eppendorf, Hamburg 20246, Germany.

*Present address: Systems Oncology, CRUK Manchester Institute, The University of Manchester, Manchester M20 4BX, UK.

‡Authors for correspondence (k.matter@ucl.ac.uk; yasu@igm.hokudai.ac.jp)

Received 16 January 2014; Accepted 6 June 2014

Journal of Cell Science

Journal of Cell Science (2014) 127, 3425–3433 doi:10.1242/jcs.149674

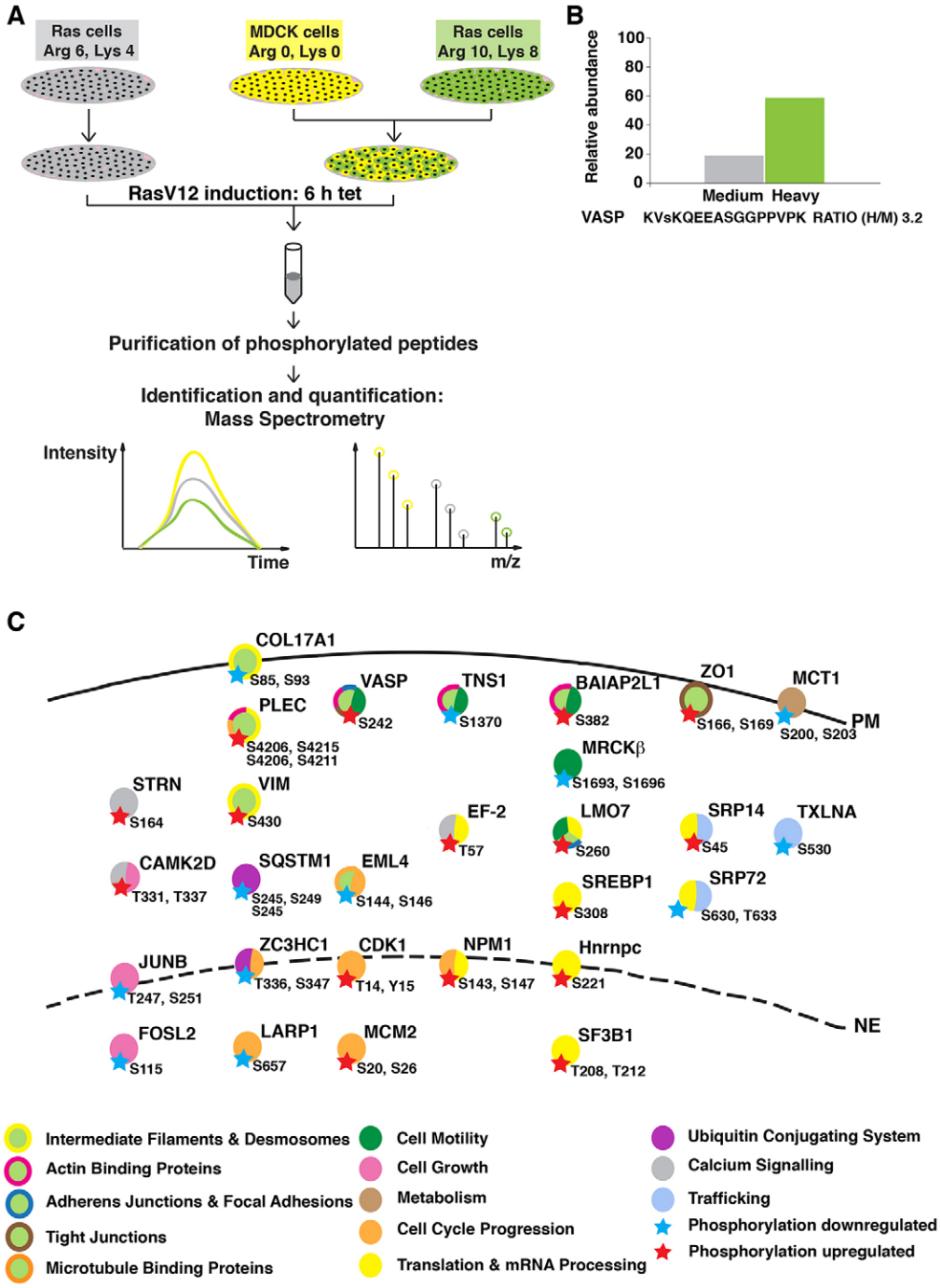

Fig. 1. Experimental outline of the SILAC screening. (A) MDCK pTR-GFP-Ras^{V12} cells were labeled with medium (Arg 6, Lys 4) or heavy (Arg 10, Lys 8) arginine and lysine, and normal MDCK cells were labeled with light (Arg 0, Lys 0) arginine and lysine. Cells were plated either as Ras cells alone or as a 1:1 mixed culture of heavy-labeled Ras:MDCK cells. After 2 h, cells were incubated with tetracycline for 6 h to induce Ras^{V12} expression. Phosphopeptides were isolated and analyzed by mass spectrometry. (B) Relative abundance of the VASP peptide from each experimental condition. The small 's' represents the detected phosphorylation site. (C) Overview of proteins in which phosphorylation was identified as being upregulated (red star) or downregulated (blue star) in Ras cells upon co-incubation with normal cells. The key known functions of the selected proteins based on Gene NCBI, UniProt and PhosphoSitePlus databases are color-coded. Abbreviations of protein names are in agreement with those listed in the Gene NCBI database. PM, plasma membrane; NE, nuclear envelope.

Ras cells mixed with normal cells as compared with their phosphorylation in Ras cells cultured alone. We found a number of proteins involved in cytoskeletal rearrangements and cell motility, as well as proteins that function in basic cellular processes such as cell cycle, cell growth and membrane biogenesis.

Induction of VASP phosphorylation in Ras-transformed cells surrounded by normal cells

The actin cytoskeleton is dramatically rearranged when Ras-transformed cells are extruded (Hogan et al., 2009). In the SILAC screening, we found that the phosphorylation of vasodilator-stimulated phosphoprotein (VASP) at serine 242 (serine 239 for the human ortholog) was upregulated (Fig. 1B,C; supplementary material Fig. S1A). VASP is a member of the Ena/VASP family of actin cytoskeleton regulators. It bundles actin fibers and, by antagonizing the capping of elongating filaments, promotes actin polymerization (Barzik et al., 2005; Bear et al., 2002; Hansen and Mullins, 2010; Hüttelmaier et al., 1999; Pasic et al., 2008). The protein localizes at sites of high actin turnover, including lamellipodia and filopodia, where it promotes actin polymerization and regulates the geometry of F-actin networks (Benz et al., 2009; Lanier et al., 1999; Rottner et al., 1999; Scott et al., 2006). VASP is a well-established target of protein kinases, and human VASP harbors three major phosphorylation sites – serine 157 (S157), serine 239 (S239) and threonine 278 (T278) (Benz et al., 2009; Blume et al.,

Journal of Cell Science (2014) 127, 3425–3433 doi:10.1242/jcs.149674

2007; Butt et al., 1994). The first two sites are phosphorylated by the cAMP- and cGMP-dependent protein kinases (PKA and PKG, respectively), whereas the AMP-activated protein kinase (AMPK) phosphorylates T278. Functionally, these serine/threonine phosphorylations impair the actin polymerization and anti-capping activities of VASP and control its subcellular targeting (Benz et al., 2009; Blume et al., 2007). Given the importance of the actin cytoskeleton for cell shape changes and for apical extrusion of transformed cells, we examined the functional significance of VASP phosphorylation.

As we were not able to detect the S242 phosphorylation of endogenous VASP by immunofluorescence, we produced Ras cells stably expressing His-tagged wild-type VASP (Ras-VASP-WT; supplementary material Fig. S2A). When Ras-VASP-WT cells were co-cultured with normal cells, we observed enhanced immunostaining for VASP phosphorylated at S239 (pVASP) compared with that observed in Ras-VASP-WT cells cultured alone (Fig. 2A; supplementary material Fig. S2B). Previously, we reported that, prior to apical extrusion, the height of Ras cells along the apico-basal axis significantly increased compared with the height of the surrounding normal cells (Hogan et al., 2009). Here, we found that the increased amount of pVASP was closely correlated with that cell shape change in Ras cells surrounded by normal cells (Fig. 2B), suggesting that the phosphorylation of VASP is involved in the process of apical extrusion.

To quantify pVASP, we immunoprecipitated exogenous VASP proteins from Ras-VASP-WT cells that were cultured alone (Alo) or co-cultured with normal cells (Mix), using an anti-His-tag antibody. We found that pVASP was increased twofold under the mixed culture condition (Fig. 2C,D). The difference in pVASP was also detected in the total cell lysates where both endogenous and exogenous VASP proteins were present (Fig. 2C,E) or when only endogenous VASP was analyzed (supplementary material Fig. S2C). The timing of the increase in pVASP (16–20 h after the induction of Ras^{V12} expression) was correlated with the time of extrusion (Fig. 2E; supplementary material Fig. S2C). When Ras^{V12} expression was not induced (i.e. in the absence of tetracycline), the increase in pVASP was not observed under the mixed culture condition (supplementary material Fig. S2D), suggesting that the non-cell-autonomous upregulation of pVASP is dependent on Ras^{V12} expression. Thus, VASP is differentially phosphorylated in Ras-transformed cells mixed with normal cells at a time when the actin cytoskeleton is reorganized and the cell shape is altered.

Phosphorylation of VASP promotes apical extrusion

To test the role of VASP, we depleted VASP in Ras cells using RNA interference (Fig. 3A,B). When VASP-knockdown Ras cells were surrounded by normal cells, apical extrusion was significantly enhanced (Fig. 3C,D). Expression of exogenous wild-type VASP rescued the knockdown phenotype (Fig. 3E; supplementary material Fig. S2E). By contrast, expression of the phosphomimetic mutant (S239D) of VASP did not complement the knockdown phenotype, and a partial rescue was obtained by expression of the non-phosphorylatable mutant (S239A) (Fig. 3E). The lack of rescue was not due to the lower expression levels of the mutant proteins (data not shown). No extrusion was observed when VASP was depleted in non-transformed pTR-GFP cells cultured in the presence of normal MDCK cells (supplementary material Fig. S2F). When the expression of GFP–Ras^{V12} was not induced, the presence of wild-type VASP did not result in cell extrusion (supplementary material Fig. S2G). These data indicate that VASP plays an inhibitory role in the apical extrusion of transformed cells and that phosphorylation of VASP at S239 relieves its suppressive effect. The lack of a complete rescue by the non-phosphorylatable mutant might be due to the necessity for the spatiotemporal regulation of VASP phosphorylation.

It was previously reported that phosphorylation of VASP at S239 induces a rounded cell shape and prevents the formation of various types of protrusions (Lindsay et al., 2007; Zuzga et al., 2012). To investigate whether VASP phosphorylation had a comparable effect in Ras cells, we cultured cells at low density, allowing them to spread, and analyzed the effect of the expression of VASP on cell morphology. Overexpression of VASP S239D reduced the formation of lamellipodia, prevented spreading and promoted a compact cell shape (supplementary material Fig. S2A,H). We next analyzed VASP-knockdown Ras cells expressing the exogenous wild-type or mutant forms of VASP proteins. VASP knockdown in Ras cells inhibited cell spreading and, consequently, decreased the average planar surface of the cells, and the expression of VASP S239D in depleted cells further promoted this phenotype, suggesting that the mutant form of VASP acted in a dominant-negative manner and blocked the endogenous VASP that was still expressed in the knockdown cells (supplementary material Fig. S2A,I). Conversely, expression of wild-type VASP or VASP S239A increased cell spreading (supplementary material Fig. S2A,I). When the expression of GFP–Ras^{V12} was not induced, the presence of wild-type VASP did not significantly alter cell spreading (supplementary material Fig. S2J). Although the knockdown of VASP suppressed the initial formation of cell adhesions, the expression of VASP or VASP mutants complemented this phenotype equally, suggesting that phosphorylation does not affect initial adhesion rates (supplementary material Fig. S2K). These data indicate that VASP phosphorylation regulates the cell shape of Ras-transformed cells.

PKA regulates VASP phosphorylation in Ras-transformed cells in a non-cell-autonomous manner

The expression of Ras^{V12} induced a temporal increase in the amount of phosphorylated (p)VASP (supplementary material Fig. S3A), which was further enhanced when Ras cells were co-cultured with normal cells (Fig. 2A,C–E). To identify the responsible kinase, we examined the involvement of PKG, which phosphorylates S239 in various cell types (Becker et al., 2000; Benz et al., 2009; Zuzga et al., 2012). However, the PKG inhibitor Rp-8-Br-PET-cGMPS did not affect the phosphorylation of VASP in Ras cells (Fig. 4A; supplementary material Fig. S3B). Similarly, an inhibitor of nitric oxide synthase (NOS), an enzyme that often functions upstream of PKG and pVASP, did not suppress VASP phosphorylation (data not shown). Another kinase that phosphorylates VASP at S239 is PKA (Smolenski et al., 1998). Treatment with the PKA inhibitor H89 strongly reduced the amount of pVASP (Fig. 4A; supplementary material S3C,D). A different PKA inhibitor, KT5720, also suppressed pVASP (supplementary material Fig. S3E). By contrast, the PKA activator DBcAMP increased pVASP levels (Fig. 4B). Collectively, these data indicate that PKA regulates the phosphorylation of VASP in Ras-transformed cells. PKA has also been reported to phosphorylate VASP S157, which leads to decreased mobility of VASP in SDS-PAGE gels (Smolenski et al., 1998). Two bands were detected by western blotting with the anti-VASP antibody, and the upper band (with reduced

Journal of Cell Science (2014) 127, 3425–3433 doi:10.1242/jcs.149674

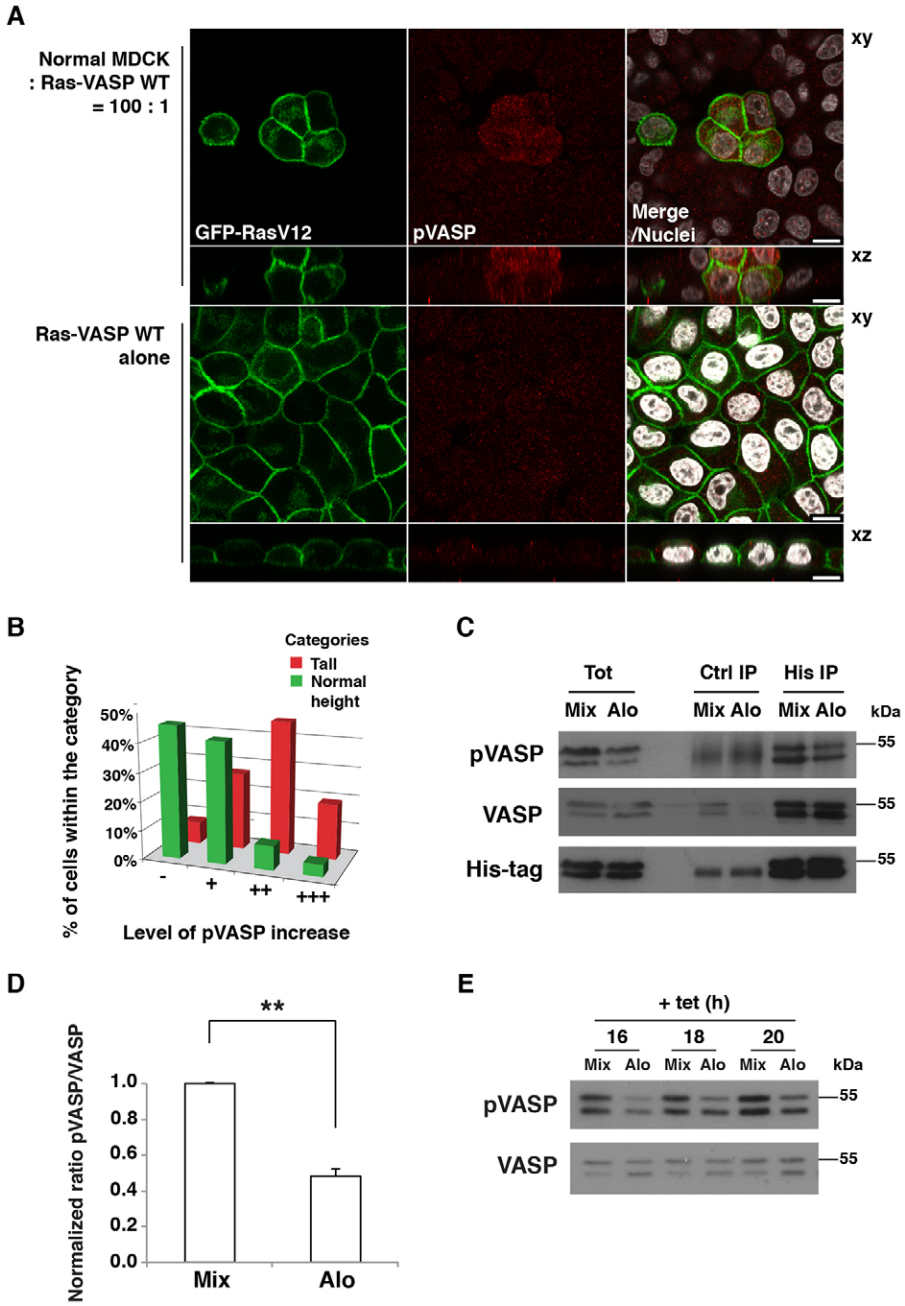

Fig. 2. Phosphorylation of VASP at S239 is increased in Ras^{V12}-transformed cells interacting with normal cells.
(A) Immunofluorescence of phosphorylated S239 of VASP in MDCK pTR-GFP-Ras^{V12}-VASP-WT cells co-cultured with normal cells (upper panels) or cultured alone (lower panels) on collagen gels. Cells were stained with antibody against phosphorylated (p)S239-VASP (red) and Hoechst 33342 (white). Scale bars: 10 μm. (B) Correlation between the levels of pS239 VASP and cell height of Ras-VASP-WT cells surrounded by normal cells. Cells were divided into two categories according to their cell shape; tall and normal height (52% and 48% of all quantified cells, respectively). Within each category, cells were classified according to their pS239 VASP level as '−' (no visible increase), '+' (slight increase), '++' (considerable increase) and '+++' (strong increase).
(C) Immunoprecipitation of VASP. Ras-VASP-WT cells and normal cells were co-cultured (Mix) or cultured alone and the respective cell lysates were mixed (Alo). Western blotting was performed with the indicated antibodies. Tot, total cell lysate; Ctrl, control. (D) Quantification of the ratio of pVASP:VASP in the total cell lysates. Values are expressed as a ratio relative to that of Mix. Data show the mean±s.d. (three independent experiments); $^{**}P<0.005$. (E) Time course of pVASP induction. Cells were cultured as described in C, and Ras^{V12} expression was induced for the indicated times. Cell lysates were examined by western blotting. After plating, the cells were cultured for 2 h (A–D) (in the same way as for the SILAC screening) or 20–24 h (E) prior to tetracycline addition.

mobility in SDS-PAGE) was more pronounced in mixed cultures and was diminished by the treatment with the PKA inhibitor (Fig. 4A,C), suggesting that phosphorylation on S157 was likewise regulated in Ras-transformed cells co-cultured with normal cells. We next asked whether PKA activity could be specifically increased in Ras-transformed cells interacting with normal cells. To detect PKA activity, we used an antibody against a phosphorylated consensus sequence recognized by PKA. Western blotting data suggested that the amount of proteins detected by the antibody was higher in the mixed culture of normal and Ras cells than in the separate culture, and the amount of protein detected was decreased following treatment of the cells with PKA inhibitor (Fig. 4D,E). By immunofluorescence, PKA activity was indeed found to be elevated in Ras cells surrounded by normal cells compared with that of Ras cells that cultured alone (Fig. 4F; supplementary material Fig. S3F). Finally, we analyzed the effect of PKA inhibition or activation on the cell morphology of Ras cells. Treatment of Ras cells with a PKA inhibitor increased cell spreading and decreased apico-basal cell height, whereas treatment with a PKA activator had the opposite effect (supplementary material Fig. S3G,H). The effect of the PKA inhibitor on cell spreading was counteracted by knockdown of VASP (supplementary material Fig. S3I), indicating that PKA stimulates cell shape changes of Ras cells in a VASP-dependent manner. At present, there is no evidence to suggest that the other members of the Ena/VASP family, Mena (also known as ENAH) and EVL, also play a role in apical extrusion. EVL does not have a serine residue corresponding to VASP S239. Both Mena and EVL are expressed in MDCK cells (Sabo et al., 2001; Tang and Brieher, 2013), but our SILAC screening did not identify

Journal of Cell Science (2014) 127, 3425–3433 doi:10.1242/jcs.149674

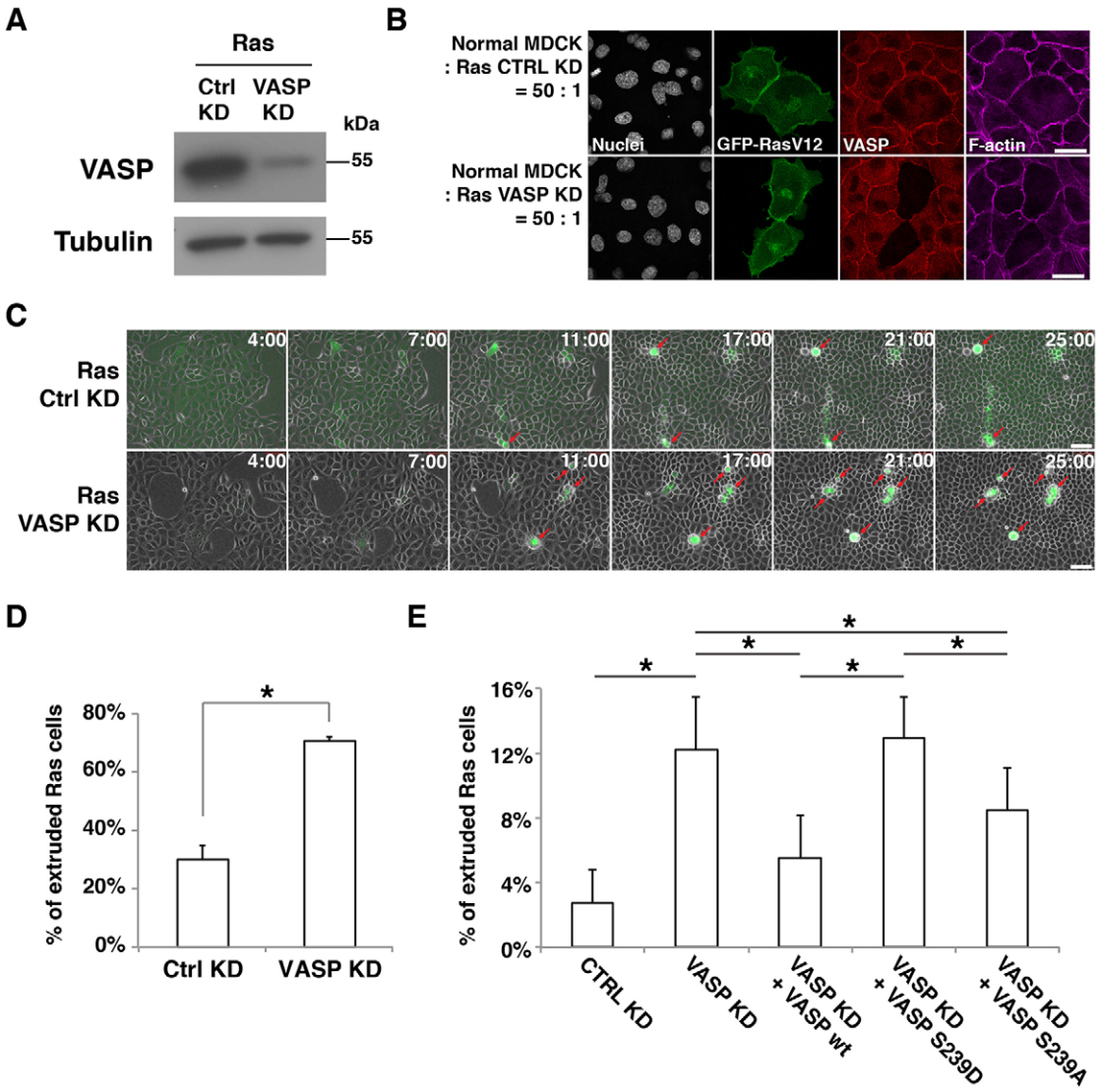

Fig. 3. Phosphorylation of VASP at S239 promotes apical extrusion. (A) Knockdown of VASP in MDCK pTR-GFP-Ras^{V12} cells. Ras cells were transfected with control siRNA (Ctrl KD) or VASP siRNA (VASP KD). Cell lysates were examined by western blotting with the indicated antibodies. (B) Immunofluorescence of VASP-knockdown Ras cells. Ras cells transfected with control siRNA or VASP siRNA were co-cultured with normal cells on glass. After induction of GFP–Ras^{V12} expression with tetracycline for 8 h, cells were stained with anti-VASP antibody (red) and Alexa-Fluor-647–phalloidin (purple). Scale bars: 25 μm. (C) Time-lapse observation of apical extrusion of Ras cells. Ras cells were transfected with control siRNA or VASP siRNA and co-cultured with normal cells on collagen gels. Images were extracted from the representative time-lapse movies, and the indicated time reflects the duration of the tetracycline treatment. Red arrows indicate extruded Ras cells. Scale bars: 50 μm. (D) Quantification of the apical extrusion of Ras cells from time-lapse analyses (25 h). Data show the mean±s.d. (two independent experiments; n=174 ctrl KD cells, n=163 VASP KD cells). (E) The effect of expression of VASP proteins in VASP-knockdown Ras^{V12}-transformed cells on apical extrusion. Ras cells were transfected with siRNAs, followed by transfection with the wild-type (wt) VASP, VASP S239D or VASP S239A construct. Note that exogenously expressed human VASP is resistant to the siRNA that targets canine VASP. The transfected Ras cells were co-cultured with normal cells, followed by tetracycline treatment for 15 h. Data show the mean±s.d. (four independent experiments; n=390 Ctrl KD cells, n=388 VASP KD cells, n=373 VASP KD+VASP WT cells, n=343 VASP KD+VASP S239D cells, n=324 VASP KD+VASP S239A cells); *P<0.05.

increased phosphorylation of Mena or EVL. In addition, knockdown of VASP substantially promoted apical extrusion. Although the possibility of an overall dosage effect of these homologous proteins cannot be ruled out, these data indicate that depletion of VASP alone is sufficient to promote extrusion.

Here, we identified a signaling pathway that drives the extrusion of Ras-transformed cells from a monolayer of normal epithelial cells; the non-cell-autonomously activated PKA–VASP pathway stimulates cell shape changes of Ras cells, which promotes their apical extrusion. VASP is a functionally important target of PKA in cell extrusion; however, it will be essential to identify other targets, as our results suggest that PKA phosphorylates multiple proteins in Ras-transformed MDCK cells (Fig. 4D,E). The activation of PKA occurred in a non-cell-autonomous fashion, indicating that Ras-transformed cells recognize and respond to the presence of normal cells, resulting in the stimulation of PKA in the transformed cells; thus, the molecular mechanism of how PKA is activated remains to be determined. Cell sorting is thought to be crucial for tissue homeostasis and development, and has been proposed to involve

Journal of Cell Science (2014) 127, 3425–3433 doi:10.1242/jcs.149674

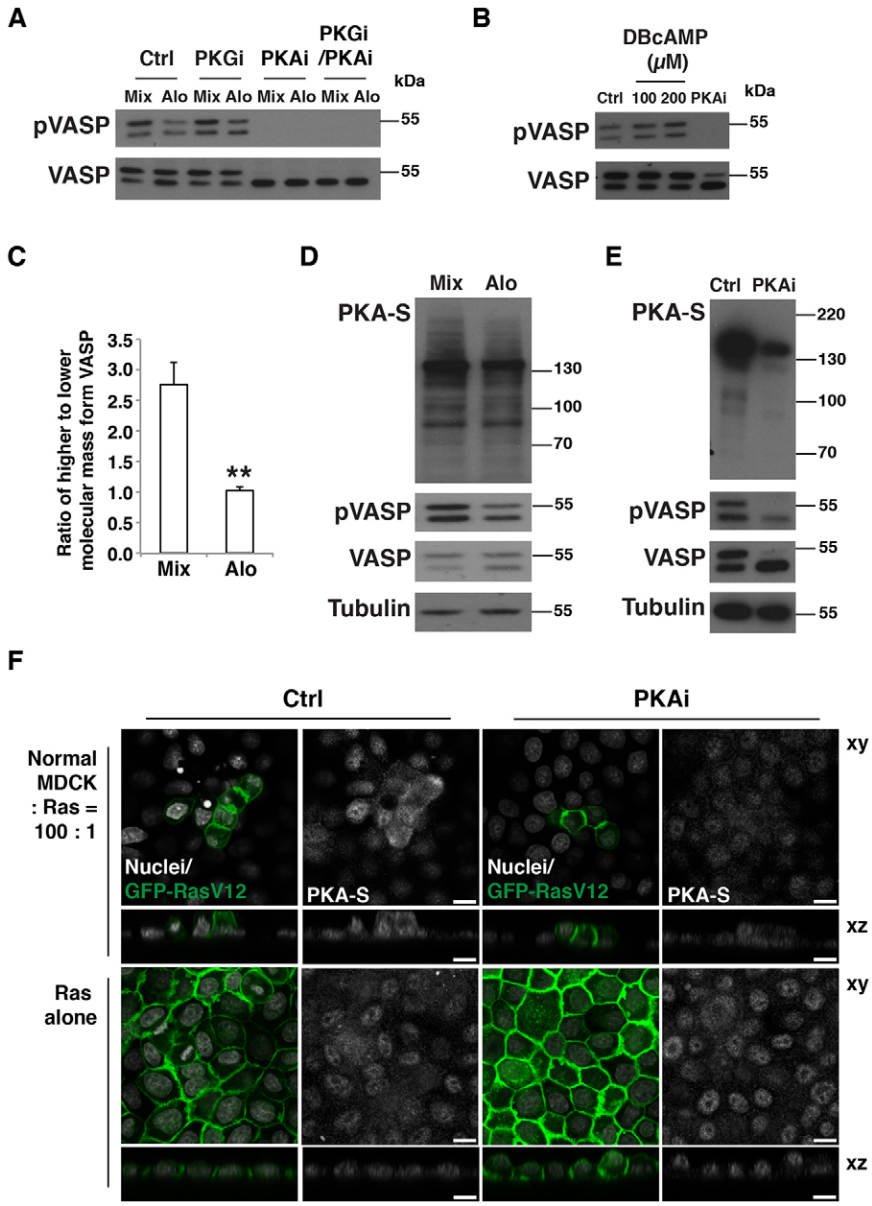

Fig. 4. PKA is a crucial regulator of the phosphorylation of VASP and the cell shape of Ras-transformed cells. (A) The effect of PKA inhibitor treatment on pS239 VASP in mixed cultures of normal and Ras cells. Ras-VASP-WT cells and normal cells were co-cultured (Mix) or cultured alone followed by mixing of the cell lysates (Alo). Cells were incubated with tetracycline for 16 h in the presence of the PKA inhibitor H89 (PKAi) and/or the PKG inhibitor Rp-8-Br-PET-cGMPS (PKGi). Cell lysates were examined by western blotting with the indicated antibodies. Ctrl, control. (B) The effect of PKA inhibitor or activator on pS239 VASP in Ras cells. Ras cells were cultured for 4 h with the PKA activator dibutyryl-cAMP (DBcAMP) at the indicated concentrations or with the PKA inhibitor H89. Cell lysates were examined by western blotting with the indicated antibodies. (C) Quantification of the effect of co-culturing Ras and normal cells on the phosphorylation of S157 VASP. After a 20-h incubation of cells with tetracycline, cell lysates were analyzed by western blotting using an anti-VASP antibody. Data show the mean±s.d. (three independent experiments); $^{**}P<0.005$. (D,E) Analyses of phosphorylated substrates of PKA in normal cells and Ras cells that were co-cultured (Mix) or cultured alone followed by mixing of the cell lysates (Alo). Cells were incubated with tetracycline for 20 h. In E, during the tetracycline treatment, cells were incubated in the absence (Ctrl) or presence (PKAi) of the PKA inhibitor H89. Cell lysates were examined by western blotting with the indicated antibodies. PKA-S, antibody against phosphorylated substrates of PKA. (F) Immunofluorescence analyses of phosphorylated substrates of PKA. Ras cells were co-cultured with normal cells (upper panels) or cultured alone (lower panels) on collagen gels. After a 20-h incubation with tetracycline in the absence or presence of H89 (PKAi), cells were stained with antibody against phosphorylated substrates of PKA and with Hoechst 33342 (white). Scale bars: 10 μm.

differences in membrane tension between cells. Apical extrusion of transformed cells can be considered to be a process of three-dimensional cell sorting, and, given their effects on the actin cytoskeleton and cell shape, PKA and VASP might regulate membrane tension at the boundary between normal and transformed cells. Understanding how this pathway is stimulated might help to improve our knowledge of the events occurring at the early stage of carcinogenesis and open new avenues to fight this life-threatening disease.

MATERIALS AND METHODS

Plasmids, antibodies and materials

pcDNA3-VASP-WT-His, pcDNA3-VASP-S239D-His and pcDNA3-VASP-S239A-His were as described previously (Benz et al., 2009). The following primary antibodies were used; rabbit anti-VASP (immunofluorescence, 1:200; western blotting 1:10,000), rabbit anti-pVASP S239 (immunofluorescence, 1:50), rabbit anti-phospho-(Ser/Thr) PKA substrates (immunofluorescence, 1:100; western blotting, 1:1000) from Cell Signaling (supplied by New England Biolabs; Hitchin, Hertfordshire, UK), mouse anti-pVASP S239 (western blotting, 1:5000) from Santa Cruz Biotechnology (Heidelberg, Germany), mouse anti-His-tag (western, blotting 1:3000) from Sigma-Aldrich (Gillingham, Dorset, UK) and mouse anti-α-tubulin as described previously (Kreis, 1987). The following secondary antibodies were used for immunofluorescence (1:300); Alexa-Fluor-647-conjugated anti-rabbit-IgG and anti-mouse-IgG antibodies from Molecular Probes by Life Technologies (Paisley, UK), Cy3-conjugated anti-rabbit-IgG and anti-mouse-IgG antibodies from Jackson ImmunoResearch Laboratories (West Grove, PA). Atto-647N–phalloidin from Sigma-Aldrich was used at 20 nM. The following inhibitors were used; PKG inhibitor Rp-8-Br-PET-cGMPS hydrate (100 nM) and NOS inhibitor L-NG-nitroarginine methyl ester (0.3 mM) from Santa Cruz Biotechnology, PKA inhibitor H89 from Cambridge Biosciences (Cambridge, Cambridgeshire, UK; at 10 μM for sparsely plated cells or 20 μM for confluent cells) and PKA inhibitor KT5720 (10 or 20 μM). The PKA activator dibutyryl-cAMP (200 mM) was from Enzo Life Sciences (Exeter, Devon, UK).

Cell culture and RNA interference

MDCK cells, MDCK pTR-GFP and MDCK pTR-GFP-Ras^{V12} cells were cultured as described previously (Hogan et al., 2009). MDCK pTR-GFP-Ras^{V12} cells expressing His–VASP-WT, His–VASP-S239D or

His–VASP-S239A were maintained in medium supplemented with 500 µg/ml of G418 (Calbiochem; supplied by Merck Millipore; Darmstadt, Germany). To induce GFP–Ras^{V12} expression, 2 µg/ml tetracycline was added to the culture medium. For immunofluorescence and time-lapse experiments, cells were cultured on type-I collagen gels from Nitta Gelatin (Nitta Cellmatrix type 1-A; Osaka, Japan) as described previously (Hogan et al., 2009). For the adhesion assay, 96-well plates were coated with 0.5 mg/ml collagen solution in 1 mM acetic acid over several hours, then dried overnight at room temperature under sterile conditions. The plates were either used immediately or stored at 4℃. For the spreading assay, cells were plated onto plastic-bottomed dishes. To establish MDCK pTR-GFP-Ras^{V12} cell lines stably expressing VASP proteins, MDCK pTR-GFP-Ras^{V12} cells were transfected with pcDNA3-VASP-WT-His, pcDNA3-VASP-S239D-His or pcDNA3-VASP-S239A-His, together with pCB6 using Lipofectamine^{TM} 2000 (Life Technologies), followed by selection in medium containing 625 µg/ml G418, 5 µg/ml blasticidin and 400 µg/ml zeocin.

Non-targeting control siRNAs and siRNAs targeting VASP were purchased from Thermo Scientific (Hemel Hempstead, Hertfordshire, UK), resuspended to a final concentration of 20 µM in 1× siRNA buffer (20 mM KCl, 0.2 mM $MgCl_2$, 6 mM HEPES/NaOH pH 7.5) and stored at −80℃. The sequence targeted by siRNA within canine VASP was 5′-GGAAATAAGATGAGGGAGA-3′, which does not occur in exogenously expressed human VASP. For siRNA transfection experiments, cells were plated on 48-well plates at 1.2×10^4 cells per well in 200 µl of medium without selective antibiotics. Then, 0.5 µl of 20 µM siRNA and 1 µl of INTERFERin (Polyplus-transfection, Berkeley, CA) were sequentially added to 50 µl of OptiMEM (Invitrogen by Life Technologies). The transfection mixture was incubated at room temperature for 25 min and applied onto the cells. After 2 days, cells were plated onto glass coverslips, collagen-coated coverslips or collagen-coated dishes. After overnight incubation, tetracycline was added to induce the expression of GFP–Ras^{V12}. Cells were then fixed with 4% paraformaldehyde (PFA) in PBS at 4–24 h after tetracycline addition or observed by time-lapse microscopy. For Fig. 3A and supplementary material Fig. S2E,I, knockdown of VASP was analyzed at 3 days after siRNA transfection. For Fig. 3E, siRNA-treated cells were further transfected with the indicated plasmids using Lipofectamine^{TM} 2000 (Invitrogen by Life Technologies). At ∼40 h after siRNA transfection, the new transfection mixtures were prepared: (1) 0.35 µg of plasmid DNA in 40 µl of OptiMEM; (2) 1 µl of Lipofectamine 2000 in 40 µl of OptiMEM. After 5 min, solutions 1 and 2 were combined and incubated for 25 min. The mixture was then applied onto the knockdown cells, and, after 8 h, cells were plated onto collagen-coated coverslips. After an overnight incubation, tetracycline was added, and, after a further 15 h, the cells were fixed with 4% PFA in PBS.

Time-lapse analyses and immunofluorescence

For each assay, between 0.8×10^6 and 1.2×10^6 cells were plated onto collagen-coated six-well plates. MDCK pTR-GFP-Ras^{V12} cells were mixed with MDCK cells at a ratio of 1:100 or 1:50 (pTR-GFP-Ras^{V12}:normal cells). After incubation for 6–16 h, tetracycline was added to induce GFP–Ras^{V12} expression. Cells were incubated for the indicated times or observed by time-lapse microscopy. For time-lapse experiments, at 4 h of tetracycline induction, cell groups smaller than four cells were chosen for observation. The behavior of each Ras cell was followed during the time-lapse observation, and the time of the respective extrusion event was recorded. Extrusion rates were quantified by dividing the number of extruded cells by the total number of cells present during the analyzed timecourse. For Fig. 2A,B, cells were incubated for 2 h after plating, followed by tetracycline addition and further incubation for 6 h (as for the SILAC screen). For immunofluorescence, cells were fixed at the indicated times with 4% PFA in PBS for 10 min. Cells were permeabilized in a solution containing 0.5% Triton X-100 and 0.3% bovine serum albumin (BSA) in PBS for 15 min, then washed once in quenching solution (20 mM glycine and 0.5% BSA in PBS) and incubated in the same solution for 30 min. Next, cells were incubated with blocking buffer (0.5% BSA and 0.2% Triton X-100 in PBS) for 1–2 h. Primary antibodies diluted in blocking buffer were applied for 2–3 h or overnight (for cells on collagen). Cells were washed three times for 10 min with blocking buffer and were incubated with fluorescently conjugated secondary antibodies and/or phalloidin for 1–3 h at room temperature. Cells were then washed three times for 10 min in blocking buffer and incubated with Hoechst 33342 (Life Technologies) in PBS for 3 min, followed by washing in PBS and mounting onto a glass slide with mowiol (Merck Millipore) when cells were cultured on collagen or with Prolong Gold Antifade Reagent (Life Technologies) when cultured on glass. For immunofluorescence of phosphorylated proteins, PBS was replaced with TBS containing phosphatase inhibitors (1 mM sodium orthovanadate, 0.1 mM ammonium molybdate and 10 mM sodium fluoride).

Time-lapse analyses were performed using a Zeiss Axiovert 200 M Microscope with a Hamamatsu Orca AG camera using 20×/0.5 or 20×/0.4 air objectives (Carl Zeiss NTS in Cambridge, Cambridgeshire, UK) or a Nikon Eclipse Ti-E with a CoolSNAP HQ2 camera using a 10×/0.45 air objective (Nikon Instruments Europe; Kingston upon Thames, Surrey, UK). Images were captured and analyzed using Volocity 6.2.1 software (PerkinElmer; Waltham, MA) or NIS-Elements software 4.0 (Nikon, Tokyo, Japan), respectively. Fixed immunofluorescence samples were analyzed with a Leica SPE3 DM4000 with a single PTM using a 63×/1.3 oil objective (Leica Microsystems; Wetzlar, Germany). Images were captured and analyzed using Leica Application Suite (LAS) software. Pixel intensity was quantified using ImageJ 1.48 (Fiji) digital analysis software (National Institutes of Health; Bethesda, MD). Cell boundaries in *xz* confocal sections were outlined using the actin channel, and this region was used to measure average pixel intensity in the PKA-S channel. Cells were counted following 15 h of tetracycline treatment.

Adhesion assay and spreading assay

For the adhesion assay, cells were suspended at a concentration of 0.5×10^6 cells/ml in DMEM containing 1% BSA, and 50 µl of cell suspension was added onto collagen-coated 96-well plates in a total volume of 200 µl, followed by incubation for 30 min. Unattached cells were then removed by three consecutive PBS washes. Attached cells were fixed and stained with 1% Crystal Violet in 20% methanol for 15 min. Excess dye was removed by five washes with water. Crystal Violet trapped in the cells was extracted with 300 µl of 1% SDS in PBS, and the absorbance was measured at 570 nm using FLUOstar OPTIMA microplate reader (BMG Labtech; Ortenberg, Germany). Cell numbers were normalized to protein concentrations measured using Precision Red reagent (Cytoskeleton; Denver, CO) in the microplate reader according to the manufacturer's protocol. For the spreading assay, at 24 h after plating, tetracycline was added with or without PKA inhibitor, and cells were analyzed after 4 h or observed for 24 h by time-lapse microscopy. Cell images were analyzed using ImageJ 1.48 (Fiji) digital analysis software, and the planar cell surface was calculated.

Western blotting and immunoprecipitation

For western blotting, $0.1–0.2\times10^6$ cells were plated onto 48-well plates. Three conditions were used; (1) normal MDCK cells alone, (2) MDCK pTR-GFP-Ras^{V12} cells alone and (3) a 1:1 mixed population. Tetracycline was added either 8–10 h after plating or after an overnight incubation. Inhibitors were added with tetracycline for 16–24 h. Cells from each well of conditions 1 and 2 were combined for 'Alone' fractions, whereas 'Mixed' fractions were from two wells of condition 3. Western blotting data were quantified using ImageJ software. For immunoprecipitation, cells were plated as normal MDCK cells alone, MDCK pTR-GFP-Ras^{V12} cells alone or a 1:1 mixed population at 4.0×10^8 cells per 15-cm plate. Tetracycline was added at 2 h after plating. After 6 h, cells were washed with ice-cold PBS and harvested in 1 ml GB buffer (10 mM HEPES/NaOH pH 7.4, 150 mM NaCl, 1% Triton X-100, 0.5% sodium deoxycholate and 0.2% sodium dodecylsulfate) containing 5 µg/ml leupeptin, 50 µM phenylmethylsulfonylfluoride, 7.2 trypsin inhibitor units of aprotinin, 50 ng/ml benzamidine, 10 ng/ml pepstatin A and phosphatase inhibitors (1 mM sodium orthovanadate, 0.1 mM ammonium molybdate, 10 mM sodium fluoride and 24 nM calyculin A). Samples were homogenized with a syringe (needle of 25 G) and incubated with

prewashed Sepharose beads for 30 min at 4℃. After centrifugation at 14,000 ***g*** for 10 min at 4℃, 50 µl of the precleared supernatants were taken as the 'Tot' fraction (total cell lysate). The rest of the supernatants were subjected to immunoprecipitation for 2 h with 50 µl of prewashed Protein G beads conjugated with 2 µg of control mouse IgG or anti-His-tag antibody. The beads were subsequently washed twice with GB buffer and once with PBS. Bound proteins were eluted with 100 µl of SDS-PAGE sample buffer for 10 min at 99℃, followed by western blotting.

Data analyses

Two-tailed Student's *t*-tests were used to determine *P*-values.

SILAC labeling combined with mass spectrometry

Medium preparation

Medium for SILAC labeling was prepared as follows; 13.26 g of arginine- and lysine-deficient DMEM powder (Caissons Laboratories; North Logan, UT) was mixed with 3.7 g of sodium bicarbonate and dissolved in 1 litre of ultrapure autoclaved water. The pH was adjusted to 7.1, and the medium was filtered. Before culturing MDCK cells, the medium was supplemented with dialyzed fetal bovine serum (30 MWCO) (Life Technologies), as well as penicillin-streptomycin and GlutaMax (Life Technologies). Labeled amino acids (Sigma-Aldrich) were added at a final concentration of 50 µg/l as follows: for a 'light' label, lysine-0 (unlabeled) and arginine-0 (unlabeled); for a 'medium' label, lysine-4 ($[^2D_4]$-labeled) and arginine-6 ($[^{13}C_6]$-labeled); for a 'heavy' label, lysine-8 ($[^{13}C_6]$, $[^{15}N_4]$-labeled) and arginine-10 ($[^{13}C_6]$, $[^{15}N_4]$-labeled).

Labeling of Ras and MDCK cells

MDCK and two sets of Ras cells were labeled for five generations in SILAC medium with light, heavy and medium amino acids, respectively. The labeling efficiency was calculated from mass spectrometric analysis of labeled lysates. In short, cell lysates were mixed (heavy:light in a 1:1 ratio or medium:light in a 1:1 ratio) and separated by SDS-PAGE. Two gel bands of high and low molecular mass were excised, digested and analyzed by liquid chromatography-mass spectrometry (LC-MS). Relative quantification of the heavy:light ratio and medium:light ratio in these proteins revealed a labeling efficiency of 98% for both arginine and lysine isotopic labels.

Cell culture and lysis

Cells were plated at 4×10^7 cells per 15-cm plate. Medium-labeled Ras cells were plated alone on two plates, and heavy-labeled Ras cells were mixed at a 1:1 ratio with light-labeled MDCK cells on four plates. The high cell density ensured that cells reattached and re-established junctions rapidly. All the cells were then cultured in light medium for 2 h, and, after tetracycline addition, cells were further incubated in light medium for 6 h. We confirmed that, during the 8 h incubation in light medium, label exchange was not higher than 10–20%. Cells were washed with TBS and lysed in 10 ml of 100 mM Tris-HCl pH 8.0, 9 M urea and 0.2 mM sodium vanadate. The cell lysates were combined in a tube and sonicated (three rounds of 15 s each). After spinning down for 10 min at 10,000 ***g***, the supernatant was collected in a fresh tube. To reduce disulfide bonds, dithiothreitol (DTT) was added to a final concentration of 5 mM, followed by incubation at 55℃ for 15 min. After cooling down, the alkylating agent iodoacetamide was added to a final concentration of 10 mM, and the tube was incubated for a further 15 min in the dark. Finally, the lysates were topped up to 45 ml with 100 mM Tris-HCl pH 8.0, and 20 µg of trypsin was added at a 1:100 ratio. After digestion for 48 h, the obtained peptides were kept at 4℃.

Purification of peptides and isolation of phosphopeptides

Sep-Pak C18 Plus Short Cartridges (Waters; Milford, MA) were used to purify peptides. The column was activated by the application of 5 ml of acetonitrile (MeCN) and washed twice with 7 ml of 0.1% trifluoroacetic acid (TFA). TFA was added to the peptide solution at a final concentration of 1%. The lysate was then spun down at 5000 ***g*** for 5 min, and the supernatant was loaded onto the column. The column with bound peptides was subsequently washed twice with 10 ml of 0.1% TFA. Peptides were eluted with 8 ml of a solution containing 50% MeCN and 0.1% TFA (50% MeCN/0.1% TFA), and the eluates were frozen for ≥30 min on dry ice and finally dried in a Savant SC250EXP SpeedVac concentrator (Thermo Scientific). For the isolation of phosphopeptides, dried peptide pellets were resuspended in 25% MeCN/0.1% TFA to a concentration of 20 mg/ml. Phosphorylated peptides were purified using Phos-Select Iron Affinity gel (Sigma-Aldrich). A total of 300 µl of the beads were washed with 0.1% TFA, followed by two washes with 25% MeCN/0.1% TFA. 100 µl of the peptide solution (2 mg of peptides) was diluted to a concentration of 5 mg/ml in 150 µl of 25% MeCN/0.1% TFA and applied onto the gel for 2 h with rotation at room temperature. The gel with bound phosphorylated peptides was then spun down for 30 s at 800 ***g*** and washed as follows; twice with 0.1% TFA, once with 0.1% TFA/50% MeCN, twice with 1% TFA/50% MeCN and, finally, once with ultrapure water. The elution was performed twice with 250 µl of 100 mM ammonium bicarbonate (pH 9.5) for 10 min at room temperature. Eluted fractions were combined and acidified with 20 µl of 20% TFA, frozen on dry ice for 30 min and dried in a vacuum centrifuge.

Hydrophilic-interaction liquid chromatography

Phosphorylated peptides isolated from 10 mg of total peptides were resuspended in 500 µl of 80% MeCN prior to injection, and fractionated using hydrophilic-interaction liquid chromatography (HILIC) (Ultimate 3000 HPLC system, Thermo Scientific). The following solvents were used; A (0.005% TFA), B (90% CAN/0.005% TFA) and C (0.04% TFA). Samples were loaded in 90% solvent B on a 2.1×150-mm TSKgel Amide 80 column (Hichrom; Theale, Berkshire, UK). The following gradient steps were performed; 100% B for 3 min, to 90% B over 2 min, to 70% B over 20 min, to 20% over 10 min, while solvent C increased from 0 to 20%. Between 12 and 44 min, 16 fractions (300 µl each) were collected and lyophilized for LC-MS analyses.

Liquid chromatography tandem mass spectrometry

Phosphorylated peptides were identified by using liquid chromatography tandem mass spectrometry (LC-MS/MS) using nanoflow capillary reversed-phase liquid chromatography on an Eksigent NanoLC-Ultra 2D with a cHiPLC-nanoflex system (Eksigent, Dublin, CA) coupled to an LTQ Orbitrap Velos mass spectrometer (Thermo Scientific). A 'trap and elute' configuration was chosen on the NanoFlex system, and two types of columns were used – a trap column (200 µm×0.5 mm) and an analytical column (200 µm×15 cm), both packed with ChromXP C18-CL 3 µm 120 Å. Samples dried after HILIC were resuspended in 10 µl of 0.1% formic acid (FA) and loaded at a flow rate of 5 µl/min for 5 min. Elution was performed at a flow rate of 300 nl/min in a linear gradient of 5% to 30% of MeCN, 0.1% FA solution over 120 min. Data-dependent mode switching automatically between Orbitrap mass spectrometry and tandem mass spectrometry acquisition was used. Acquisition of survey full scan mass spectrometric spectra (from m/z 400 to 2000) was performed in the Orbitrap Velos using a resolution of 30,000 at m/z 400. Isolation and fragmentation of the ten most intense ions with charge states >2 was performed to a value of 3×10^4 in a higher energy collision dissociation (HCD) cell. Normalized collision energy was set at 42%. Fragments were detected in the Orbitrap with a resolution of 7500. Ions were selected up to 2000 counts while ion accumulation times reached a maximum of 500 ms for full scans and 400 ms for HCD. Fragmented peptides were excluded for a duration of 60 s.

Data analyses

Peptide identification was performed using raw data obtained in Xcalibur software (Thermo Scientific) through processing in Proteome Discover v1.3 software (Thermo Scientific) with the Mascot v2.2 search engine (Matrix Science; Boston, MA) and the Ensembl dog database. The following Mascot search parameters were used: precursor mass tolerance, 10 ppm; fragment mass tolerance, 0.6 Da; trypsin missed cleavage, 2; static modifications, carbamidomethylation (C); variable modifications, oxidation (M), deamidated (NQ), phosphorylation (STY), arginine $^{13}C_6$

(R6), arginine $^{13}C_6{}^{15}N_4$ (R10), lysine $^{2}HD_4$ (K4) and lysine $^{13}C_6{}^{15}N_4$ (K8). Filters applied to obtained peptide sequence matches (PSMs) were as follows; a mascot significance threshold of ≥ 0.05, a peptide score of ≥ 20, peptide maximum rank of 1 and pRS phosphorylation site probabilities $\geq 85\%$ (PhosphoRS1.0). The false discovery rate (FDR) was set to a q-value of ≤ 0.01 (Percolator) for peptides. Identified peptides with a heavy:medium ratio >1.5 or <0.5 in any of the three performed experiments were chosen for a preliminary search, and the ratios were compared between experiments. Phosphorylated peptides for which a heavy:medium ratio was reproduced in two repeats were chosen for further analysis. The identity of chosen peptides was confirmed by comparing them against the dog protein database with Basic Local Alignment Search Tool (BLAST, National Center for Biotechnology Information; Bethesda, MD). Identified phosphorylation sites were aligned to sites in human, mouse and rat proteins. Current knowledge concerning the characterization of these sites (regulators, function) was obtained from the PhosphoSitePlus database (Cell Signaling; Boston, MA) website and literature in the database (NCBI).

Acknowledgements
We thank Patric Turowski (UCL, London, UK), John Garthwaite (UCL, London, UK) and Catherine Hogan (Cardiff University, Cardiff, UK) for advice and contribution of reagents.

Competing interests
The authors declare no competing interests.

Author contributions
K.A.A. performed the experiments and analyzed the results. K.A.A., K.M. and Y.F. conceived the experiments and wrote the manuscript. K.A.A., C.J. and Y.F. designed the SILAC screen. J.S. performed HILIC and LC-MS/MS. A.O., M.K., S.I. and M.B contributed to different aspects of experimental work and data interpretation. P.M.B. and T.R. contributed to VASP constructs. K.M. and Y.F. contributed equally to this work.

Funding
K.A.A. was supported by a fellowship from the Medial Research Council. T.R. received support from Vetenskapsrådet [grant number 21462]; the German Research Society [grant number SFB 841]; and the European Research Council [grant number ERC-StG-2012-311575_F-12]. C.J. is supported by a Cancer Research UK Career Establishment Award [grant number A12905]. K.M. and M.S.B. were supported by the The Wellcome Trust [grant numbers 084678/Z/08/Z and 099173/Z/12/Z]; and the Biotechnology and Biological Sciences Research Council. Y.F. is supported by Next Generation World-Leading Researchers (NEXT Program); the Takeda Science Foundation; the Uehara Memorial Foundation; Daiichi-Sankyo Foundation of Life Science; and Naito Foundation. Deposited in PMC for release after 6 months.

Supplementary material
Supplementary material available online at
http://jcs.biologists.org/lookup/suppl/doi:10.1242/jcs.149674/-/DC1

References
Barzik, M., Kotova, T. I., Higgs, H. N., Hazelwood, L., Hanein, D., Gertler, F. B. and Schafer, D. A. (2005). Ena/VASP proteins enhance actin polymerization in the presence of barbed end capping proteins. *J. Biol. Chem.* **280**, 28653-28662.

Bear, J. E., Svitkina, T. M., Krause, M., Schafer, D. A., Loureiro, J. J., Strasser, G. A., Maly, I. V., Chaga, O. Y., Cooper, J. A., Borisy, G. G. et al. (2002). Antagonism between Ena/VASP proteins and actin filament capping regulates fibroblast motility. *Cell* **109**, 509-521.

Becker, E. M., Schmidt, P., Schramm, M., Schröder, H., Walter, U., Hoenicka, M., Gerzer, R. and Stasch, J. P. (2000). The vasodilator-stimulated phosphoprotein (VASP): target of YC-1 and nitric oxide effects in human and rat platelets. *J. Cardiovasc. Pharmacol.* **35**, 390-397.

Benz, P. M., Blume, C., Seifert, S., Wilhelm, S., Waschke, J., Schuh, K., Gertler, F., Münzel, T. and Renné, T. (2009). Differential VASP phosphorylation controls remodeling of the actin cytoskeleton. *J. Cell Sci.* **122**, 3954-3965.

Blume, C., Benz, P. M., Walter, U., Ha, J., Kemp, B. E. and Renné, T. (2007). AMP-activated protein kinase impairs endothelial actin cytoskeleton assembly by phosphorylating vasodilator-stimulated phosphoprotein. *J. Biol. Chem.* **282**, 4601-4612.

Butt, E., Abel, K., Krieger, M., Palm, D., Hoppe, V., Hoppe, J. and Walter, U. (1994). cAMP- and cGMP-dependent protein kinase phosphorylation sites of the focal adhesion vasodilator-stimulated phosphoprotein (VASP) in vitro and in intact human platelets. *J. Biol. Chem.* **269**, 14509-14517.

Hansen, S. D. and Mullins, R. D. (2010). VASP is a processive actin polymerase that requires monomeric actin for barbed end association. *J. Cell Biol.* **191**, 571-584.

Hogan, C., Dupré-Crochet, S., Norman, M., Kajita, M., Zimmermann, C., Pelling, A. E., Piddini, E., Baena-López, L. A., Vincent, J. P., Itoh, Y. et al. (2009). Characterization of the interface between normal and transformed epithelial cells. *Nat. Cell Biol.* **11**, 460-467.

Hüttelmaier, S., Harbeck, B., Steffens, O., Messerschmidt, T., Illenberger, S. and Jockusch, B. M. (1999). Characterization of the actin binding properties of the vasodilator-stimulated phosphoprotein VASP. *FEBS Lett.* **451**, 68-74.

Jørgensen, C., Sherman, A., Chen, G. I., Pasculescu, A., Poliakov, A., Hsiung, M., Larsen, B., Wilkinson, D. G., Linding, R. and Pawson, T. (2009). Cell-specific information processing in segregating populations of Eph receptor ephrin-expressing cells. *Science* **326**, 1502-1509.

Kajita, M., Hogan, C., Harris, A. R., Dupre-Crochet, S., Itasaki, N., Kawakami, K., Charras, G., Tada, M. and Fujita, Y. (2010). Interaction with surrounding normal epithelial cells influences signalling pathways and behaviour of Src-transformed cells. *J. Cell Sci.* **123**, 171-180.

Kreis, T. E. (1987). Microtubules containing detyrosinated tubulin are less dynamic. *EMBO J.* **6**, 2597-2606.

Lanier, L. M., Gates, M. A., Witke, W., Menzies, A. S., Wehman, A. M., Macklis, J. D., Kwiatkowski, D., Soriano, P. and Gertler, F. B. (1999). Mena is required for neurulation and commissure formation. *Neuron* **22**, 313-325.

Lindsay, S. L., Ramsey, S., Aitchison, M., Renné, T. and Evans, T. J. (2007). Modulation of lamellipodial structure and dynamics by NO-dependent phosphorylation of VASP Ser239. *J. Cell Sci.* **120**, 3011-3021.

Mann, M. (2006). Functional and quantitative proteomics using SILAC. *Nat. Rev. Mol. Cell Biol.* **7**, 952-958.

Pasic, L., Kotova, T. and Schafer, D. A. (2008). Ena/VASP proteins capture actin filament barbed ends. *J. Biol. Chem.* **283**, 9814-9819.

Rottner, K., Behrendt, B., Small, J. V. and Wehland, J. (1999). VASP dynamics during lamellipodia protrusion. *Nat. Cell Biol.* **1**, 321-322.

Sabo, S. L., Ikin, A. F., Buxbaum, J. D. and Greengard, P. (2001). The Alzheimer amyloid precursor protein (APP) and FE65, an APP-binding protein, regulate cell movement. *J. Cell Biol.* **153**, 1403-1414.

Scott, J. A., Shewan, A. M., den Elzen, N. R., Loureiro, J. J., Gertler, F. B. and Yap, A. S. (2006). Ena/VASP proteins can regulate distinct modes of actin organization at cadherin-adhesive contacts. *Mol. Biol. Cell* **17**, 1085-1095.

Smolenski, A., Bachmann, C., Reinhard, K., Hönig-Liedl, P., Jarchau, T., Hoschuetzky, H. and Walter, U. (1998). Analysis and regulation of vasodilator-stimulated phosphoprotein serine 239 phosphorylation in vitro and in intact cells using a phosphospecific monoclonal antibody. *J. Biol. Chem.* **273**, 20029-20035.

Tang, V. W. and Brieher, W. M. (2013). FSGS3/CD2AP is a barbed-end capping protein that stabilizes actin and strengthens adherens junctions. *J. Cell Biol.* **203**, 815-833.

Zuzga, D. S., Pelta-Heller, J., Li, P., Bombonati, A., Waldman, S. A. and Pitari, G. M. (2012). Phosphorylation of vasodilator-stimulated phosphoprotein Ser239 suppresses filopodia and invadopodia in colon cancer. *Int. J. Cancer* **130**, 2539-2548.